Journal of Cardiology (2008) **52**, 86—101

ELSEVIER

JOURNAL of CARDIOLOGY
Official Journal of the Japanese College of Cardiology
www.elsevier.com/locate/jjcc

ORIGINAL ARTICLE

Blood flow structure and dynamics, and ejection mechanism in the left ventricle: Analysis using echo-dynamography

Motonao Tanaka (MD, FJCC)[a,*], Tsuguya Sakamoto (MD, FJCC)[b], Shigeo Sugawara (MD)[a], Hiroyuki Nakajima (RMS)[a], Yoshiaki Katahira (MD)[a], Shigeo Ohtsuki (PhD)[c], Hiroshi Kanai (PhD)[d]

[a] *Cardiovascular Center, Tohoku Welfare Pension Hospital, Fukumuro 1-12-1, Miyagino-ku, Sendai 983-0005, Japan*
[b] *Hanzohmon Hospital, Kojimachi 1-14, Chiyoda-ku, Tokyo 102-0083, Japan*
[c] *Institute of Medical Ultrasound Technology, Yokoyama 2-12-15, Sagamihara 229-1122, Japan*
[d] *Department of Electrical Engineering, Tohoku University, Aramaki-Aoba 6-6-05 Aoba-ku, Sendai 980-8579, Japan*

Received 28 April 2008; received in revised form 15 May 2008; accepted 16 May 2008
Available online 16 July 2008

KEYWORDS
Echo-dynamography;
Flow velocity vector;
Blood flow dynamics;
Ejection mechanism;
Flow axis line;
Ventricular wall dynamics;
Velocity gradient

Summary Using our ''echo-dynamography'', blood flow structure and flow dynamics during ventricular systole were investigated in 10 normal volunteers. The velocity vector distribution demonstrated blood flow during ejection was laminar along the ventricular septum. The characteristic flow structure was observed in each cardiac phases, early, mid- and late systole and was generated depending on the wall dynamic events such as peristaltic squeezing, hinge-like movement of the mitral ring plane, bellows action of the ventricle and dimensional changes in the funnel shape of the basal part of the ventricle, which were disclosed macroscopically by using the new technology of high speed scanning echo-tomography and microscopically by the strain rate distribution measured by phase tracking method.

The pump function was reflected on the changes in the flow structure represented by the flow axis line distribution and the acceleration along the flow axis line. The acceleration of the ejection had three modes, ''A'', ''B'' and ''C'', and generated by the wall dynamic events. ''A'' appeared from the apical to the outflow area along the main flow axis line, ''B'' along the anterior mitral leaflet and the branched flow axis line, and ''C'' generated by the high speed vortex behind the mitral valve. The magnitude of the acceleration was estimated quantitatively from the velocity gradient along the flow axis line. Macroscopic and microscopic asynchrony in

* Corresponding author. Fax: +81 22 719 5166.
E-mail address: m.tanaka@jata-miyagi.org (M. Tanaka).

doi:10.1016/j.jjcc.2008.05.005

the myocardial contraction and extension appeared systematically in the local part of the ventricular wall, which was helpful for making the flow structure and for performing the smooth pump function.

Introduction

All energy involved blood flow within the cardiac chambers is supplied by myocardial contraction and extension. In these circumstances, an effective transformation of the regional part of the myocardial wall is supposed to offer the most appropriate spatial pressure distribution, which helps three-dimensional (3D) blood movement.

Up to the present time, cardiac pump function has been evaluated by global pressure and volume measurements, but the changes in the spatial distribution of the regional flux and pressure (flow dynamics) have not been analyzed in detail because of the lack of the suitable measurement technology.

To solve this problem, we evaluate quantitatively the local flow structure and dynamics using ''echo-dynamography'', which enables us to assess instantaneously flow dynamics non-invasively [1—5], especially to obtain the mapping of the flow velocity vector during individual cardiac phases and also to visualize the cardiac function.

Subjects

Ten presumably healthy volunteers aged 30—50 were the subjects. In all, information within the left ventricle (LV) was obtained as to the flow velocity, flow velocity vector, flow axis line, wall motion and other variables during each early, mid- and late systole.

Methods

Measurement of flow velocity and selection of the plane for the analysis

Commercially available ultrasonic equipment (Alolka Co. model 6500) was applied in the supine or left lateral recumbent position. The ultrasonic frequency was 3 MHz with the repetition rate of 4 kHz. Apical or parasternal two-dimensional (2D) echocardiograms were obtained by 90° sector scan.

For the most advantageous section plane, we selected flow axis plane passing through the center of the mitral and aortic orifices and including the centers of both the left ventricle (LV) and left atrium and the apex. This plane includes both inflow and outflow axes of the LV. We named this ''long axis'' plane. Normal intra-ventricular flow is ''plane symmetry'' with respect to this plane, and the rectangular ones are short axis planes.

Data obtained from both 2D echocardiogram and 2D Doppler flow velocity processed off-line using our own software of ''echo-dynamography'' were transferred to the personal computer through MO disk memory.

2D flow velocity vector mapping obtained from the Doppler flow velocity

The flow velocity vector mapping on the scanning plane was obtained by the use of echo-dynamography which has been developed by us introducing the two hydrodynamic theories of the stream function [7] and the flow function [8] and explained in details in the literature [6]. This mapping shows a cross-section picture of the 3D blood flow in the LV.

The magnitude of the flow velocity vector is shown by the length of yellow line, and the standard length as the reference is shown at the left corner of the screen. The direction is indicated by the inclination and the head is marked by the red point at the edge of the line (ref. Fig. 1 left column).

Quantitative evaluation of distribution range of the velocity vector

To quantify distribution range of the velocity vector, the contour lines of the magnitude of absolute value (red area) of the vector was superimposed on the 2D echocardiogram (ref. Fig. 1 right column). Quantification was made by measuring the interval between two contour lines.

Display of flow axis line for evaluating centralization of the power produced by the ventricular wall

The ridge line (ref. Fig. 1 right column; blue line) representing the flow axis line in the LV as well as centralization of the power was obtained in the velocity vector distribution. This ridge line was depicted by the connection of positive peak points

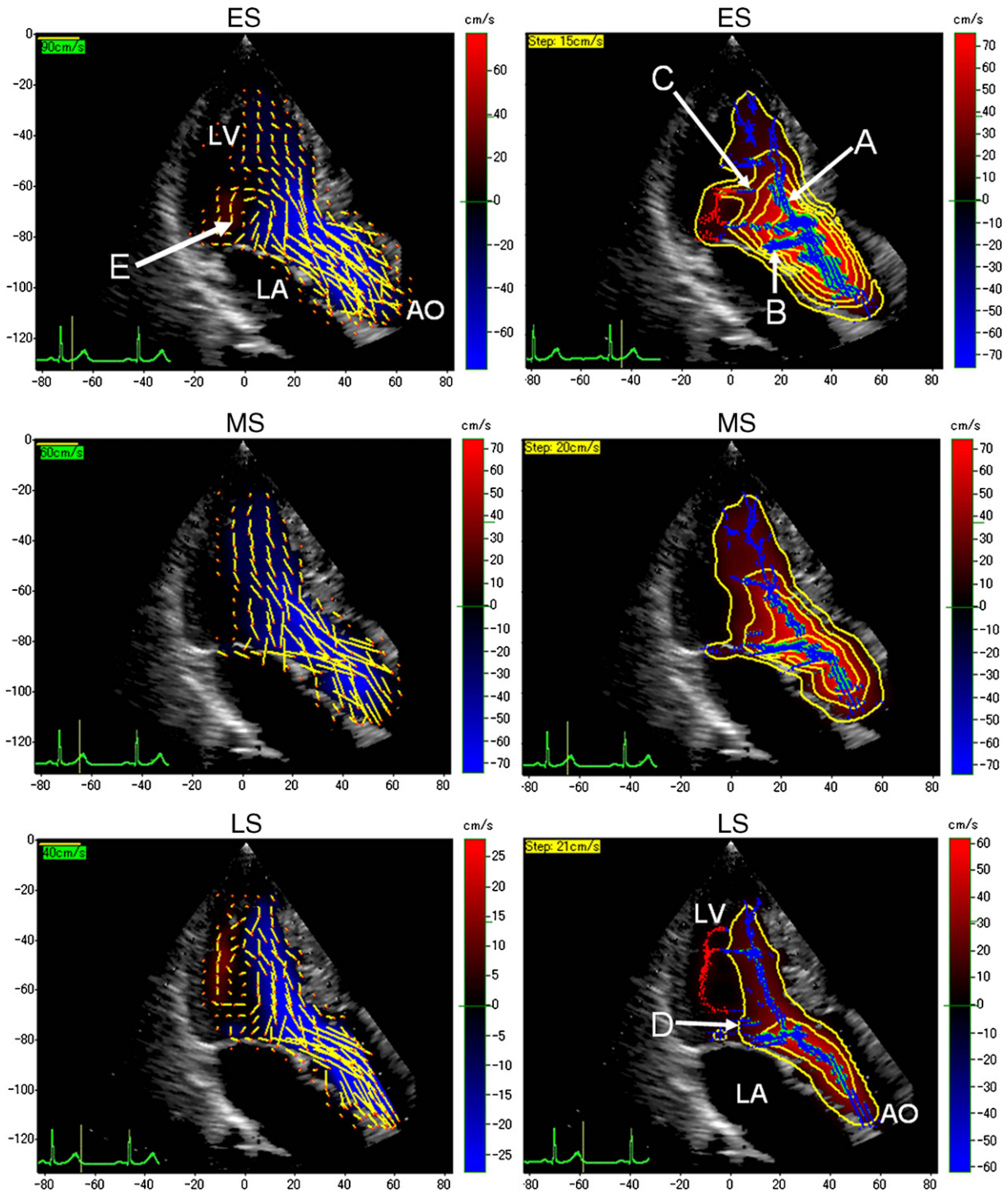

Figure 1 Left: two-dimensional (2D) mapping of flow velocity vector in systole in the longitudinal section plane of the left ventricle (LV) in a normal adult. The timing is shown in the ECG by a yellow line, and standard size of the vector by a yellow bar at the upper left corner. A white arrow (E) shows the eddy flow. ES: early systole, MS: mid-systole, LS: late systole, AO: aorta, IA: left atrium, LV: left ventricle, E: eddy. Right: 2D distribution of absolute value of velocity vector in the longitudinal plane expressed by a equi-level line (yellow line). The flow axis line distribution (blue line) during each ES, MS and LS is overlapped with the equi-level line map. An unit interval of the equi-level line is shown at the upper left side. A: acceleration A, B: acceleration B, C: acceleration C, D: deceleration.

in the absolute value of magnitude of the velocity vector and the change in the 2D pattern of the ridge line indicates local ventricular wall function [9,10].

Analysis of the LV wall movement

High-speed (66 frames/s) 2D echocardiogram was used for the analysis.

Changes in the septal and posterior wall thickness, the internal diameters at the level of each apical, central and basal area of the LV, and the diameter and displacement of the mitral valve ring (MRD and MRM) during cardiac cycle were measured macroscopically from successive 24 echocardiograms selected at every 30 ms.

Strain and strain rate in the LV wall using a new scanning technique (high frame rate sparse scan)

Thirty degree sector scan at a speed of 630 frames/s with the switching beam direction of every 5° interval (sparse scan) was performed, and measured wall thickness change microscopically in each beam direction at every thickness interval of 0.82 mm by the phase difference tracking method [11], and thus the strain rate was obtained [12,13]. Then, this was displayed on the M-mode and 2D images as color-coded information. The cold or warm color indicates wax or wane of the stain rate (ref. Figs. 5 and 6).

2D distribution of the acceleration for changing flow direction [14,15]

The direction of blood flow within the LV is greatly changed whenever ventricular wall, papillary muscles, valves and other structures are forced to displace and transform due to the wall contraction. Accordingly, measuring the ''acceleration for changing flow direction'' of the intra-ventricular blood flow, the transmitting process of the ejecting force produced by the wall contraction is possible to estimate. Then, we defined the product of the vorticity and velocity vector as the ''acceleration for changing flow direction'' [7]. This product was obtained from 2D distribution, which showed radial pattern in the eddy, and stratified pattern near the wall whenever the force is perpendicular to the blood from the ventricular wall [15] (ref. Fig. 7 left column).

Measurement of the Doppler pressure distribution [16—19]

The 3D blood flow greatly changes during ventricular contraction, particularly due to the dynamic, rather than static, pressure change. To deduce this change from the distribution of the flow velocity data on the scanning plane, the Navier—Stokes' equation of motion was applied for processing Doppler velocity data, and the theory of Helmholtz was applied to transfer velocity information to the pressure information as a scalar value [19]. The pressure depicted by the color image was overlapped on the 2D echocardiogram (ref. Fig. 7 right column). Positive and negative components are displayed as warm and cold color.

Results

Flow velocity vector distribution in the left ventricle

Typical 2D distributions of flow velocity vector during systole is shown in Fig. 1.

Early systolic phase (ES)

The distribution was wide in the basal area with large velocity gradient, while that of small gradient was seen in the anterior half area near the septum in both central and apical areas (Fig. 1ES). The vector directed from the apical area to the aorta in the anterior half of the ventricular cavity adjacent to the septum and then shifted anteriorly at the aortic area. A part of this vector separated at an adjacent area to the anterior mitral leaflet and converted posteriorly. Thus the circular arrangement of the vector was demonstrated (white arrow: E). The magnitude of the vector was minimum at the posterior half of the apical area adjacent to the posterior wall, whereas it increased rapidly toward the center of the outflow and was maximum just behind the aortic valve.

The main flow axis line (A in Fig. 1) showed a narrow ramified pattern at the apical and central areas, and the velocity gradient along this ramified flow axis line was about 5.2 in average. The flow axis line in the basal area was confluent at the outflow with the axis line (B in Fig. 1) along the anterior mitral valve and the velocity gradient was about 18.6 (Acceleration B). This was greater at the aortic area, reaching about 21.3 (Fig. 3ES). The velocities of ejected blood flow along the main flow axis line at the apical, central and basal areas were about 10, 40, and 100 cm/s, respectively. The calculated

velocity gradients in these three areas were about 4.5, 10.1 and 21.3 (Acceleration A) respectively, i.e., in the latter two areas, the velocity gradient were about two to four times bigger than that of the apical area.

Velocity vector distribution showed that the blood in the postero-apical area was stationary, while the blood flow in another areas was accelerated toward the aorta along the septum. At the same time, a part turned posteriorly, producing strong eddy just behind the mitral valve (Acceleration C) (Fig. 1). This eddy flow axis line (C in Fig. 1) joined again the main flow axis after the circular motion. The eddy was about 22 mm in diameter (D in Fig. 2), and about 56 cm/s in the circumferential speed (Fig. 2-1, bottom graph). Thus, the centrifugal force was larger than that of the eddy in the isovolumetric phase [20].

The vector in the outflow rapidly directed anteriorly toward the septum. Passing through the aortic valve, it directed posteriorly and then anteriorly again.

Mid-systolic phase (MS)

The velocity vector was observed in the anterior 2/3 areas near the left ventricular septum (Fig. 1MS) and the direction was almost straight from the apical area toward the aorta. The magnitude was extremely small in the postero-basal area, whereas it became gradually larger in the antero-basal area near the septum toward the outflow (about 100 cm/s). In the apical area the vector was about 25—30 cm/s. Circular arrangement seen

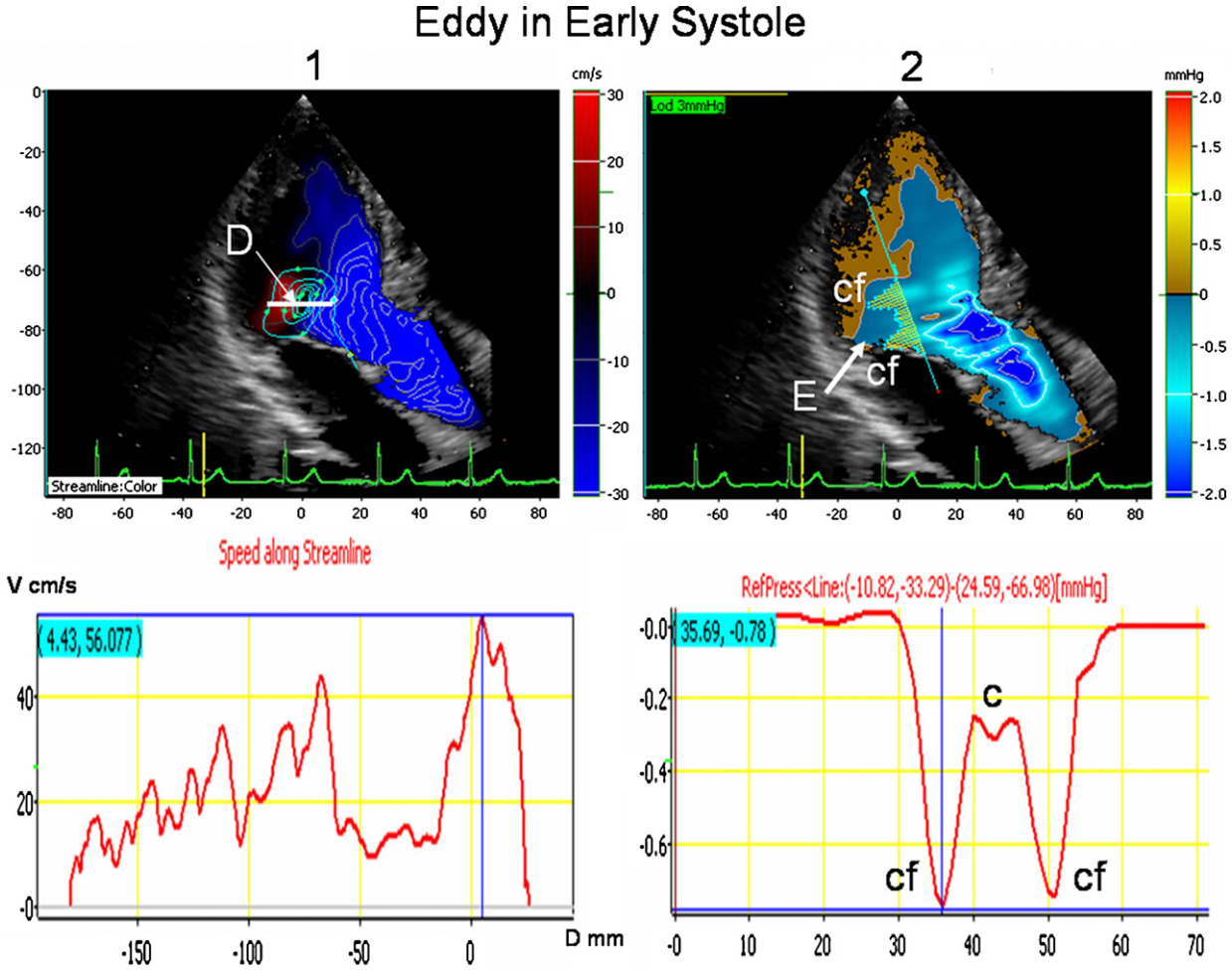

Figure 2 Measurement of the eddy in the early systolic phase—1: the diameter of the eddy using the stream line (blue line) method, which is represented by the circular stream line (D). Bottom graph shows the flow velocity along the stream line; 2: 2D distribution of the Doppler pressure (dynamic pressure) in the LV. Cold colored area shows a negative pressure and warm colored, a positive pressure. The pressure distribution on the line passing through the center of the eddy appeared in the area just behind the anterior mitral leaflet (E: white arrow) is demonstrated in the bottom graph. In a developing eddy, the pressure in a circumferential part (cf) of the eddy becomes lower than that in the center (c) of the eddy nevertheless the pressure in the eddy is negative.

in the early systolic phase under the mitral valve disappeared.

Level difference of the velocity gradient on the main flow axis line was 1.4 times greater in the central area compared to that in the apical area, and further, 2.6 times greater in the basal area compared to that of apical area. Then, velocity difference between apical and outflow areas was smaller than that in early systole (Fig. 3MS).

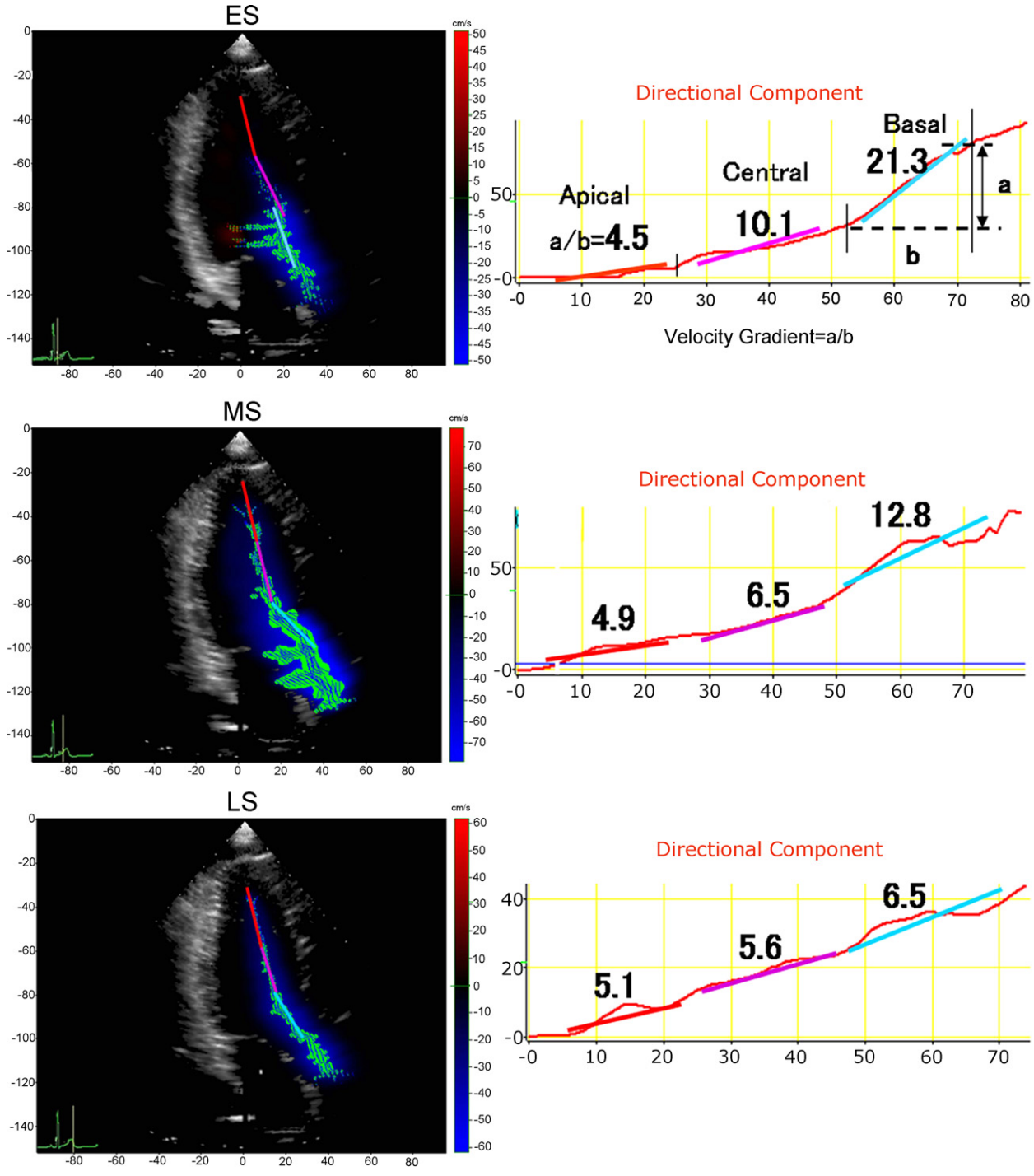

Figure 3 Velocity distribution and velocity gradient in the main flow axis line of the ejecting flow in the LV in one sample case. Left: flow axis lines of the ejection are overlapped on the color Doppler imaging. Red, pink and blue lines indicate apical, central and basal part, respectively, and the color lines correspond with the velocity gradient showing in the right column. Right: graphic display of the velocity distribution. Velocity gradient (a/b) in the three parts is demonstrated. Abscissa shows velocity in mm/s, and ordinate, distance in mm.

As seen in early systole, the main flow axis line was ramified at the apical and central areas, and the velocity gradient was about 17.2 in average. This main flow axis was parallel to the septum and gradually increased in width toward outflow area, and formed Y shape with branched line from the area just under the mitral valve, and the velocity gradient was 13.6 in average (Acceleration B).

The velocity vector of ejected blood directed anteriorly at the outflow, and directed posteriorly in the aorta (Fig. 1).

Late systolic phase (LS)

The velocity vector distributed unevenly in the anterior half area of the ventricle near the septum (Fig. 1LS). The magnitude of ejected velocity vector was about 20 cm/s, and increased slightly at the aortic orifice.

The direction of the vector was nearly parallel to the septum from the apical to basal areas, but some parts in the outflow branched to posterior direction. Then, about 1/3 to 1/6 of the ejected flow moved downward, and thereafter anteriorly, to the apical area along the ventricular inner surface (Fig. 1LS).

The velocity gradient of the branched flow axis line (D in Fig. 1LS) was about −11.1 and that of the other branched flow axis line (B in Fig. 1) was about 10.9. The velocity gradient from apical area to outflow area was almost constant (Fig. 3LS). Just under the aortic valve, blood was accelerated slightly from about 20 to 50—60 cm/s, and blood flow markedly lost the velocity in late systole.

A part of blood turned backward from the basal area toward the apical area, producing clockwise rotation along the inner surface of the posterior wall and small circular arrangement of the vector was observed in the apical area, and resulted in the deceleration of blood movement.

Displacement of the LV structures in systolic phase measured by high-speed scanning technique

Mean value in 10 normal cases are shown in Fig. 4.

Changes in the thickness of LV wall during one cardiac cycle

The thickness of the septum (IVS) increased just before the onset of the first heart sound (S1) at the apical part, whereas the increase delayed at the central and basal parts. The maximum thickness appeared in the order of the apical, central and basal part. The time difference between the apical and basal part was about 180 ms.

The thickness of the posterior wall (PW) increased about 4—6 mm during systolic phase. The onset of the increase at the apical part coincided in time with the R wave of ECG, whereas at the other two parts the increase was in early systole after transient decrease. The maximum thickness appeared in the order of the apical, central and basal part. The time difference between the apical and basal parts was about 210 ms.

Changes in internal diameter of the LV and displacement of the mitral valve structure in systolic phase

The internal diameter decreased at almost the same time of the onset of the S1 in all three parts, and the minimum was observed at apical, central and basal part in this order, showing about 60—90 ms in time differences between the apical and basal parts. The largest of the change was in the central part. The downward movement of the lateral part of the mitral valve ring (MRM) began with the onset of the S1 and continued to the end of isovolumetric relaxation. The mitral valve ring diameter (MRD) was minimal just before the onset of the S1 and increased about 10 mm during systole until the end of isovolumetric relaxation. Thus, the increase in the antero-posterior diameter of the mitral valve ring was followed by the change in the shape from oval to circular form, increasing the orifice area during systole, though the ring is fibrous tissue with little extensibility.

Strain rate distribution in the myocardium measured by sparse scan method [14—16]

Strain rate of the IVS and PW measured to analyze microscopically the myocardial mechanical events. The results were shown in Figs. 5 and 6.

Strain rate distribution in the IVS (Fig. 5)

Remarkable differences in the distribution presented in the apex between right ventricular (RV) and LV sides at the beginning (about 100 ms) and ending (about 100 ms) of systolic phase (Fig. 5-4,5). Namely, at the beginning, it increased in the LV side and decreased in the RV side, and the reverse was true at the end of systolic phase. In mid-systole, both positive and negative strain rate areas were mixed in the apical part of the IVS. In the central and basal parts, the strain rate temporarily decreased and the both parts expanded in early systolic phase. Thereafter, it increased throughout systole, and the part having large strain rate moved from RV side to LV side with the progress of sys-

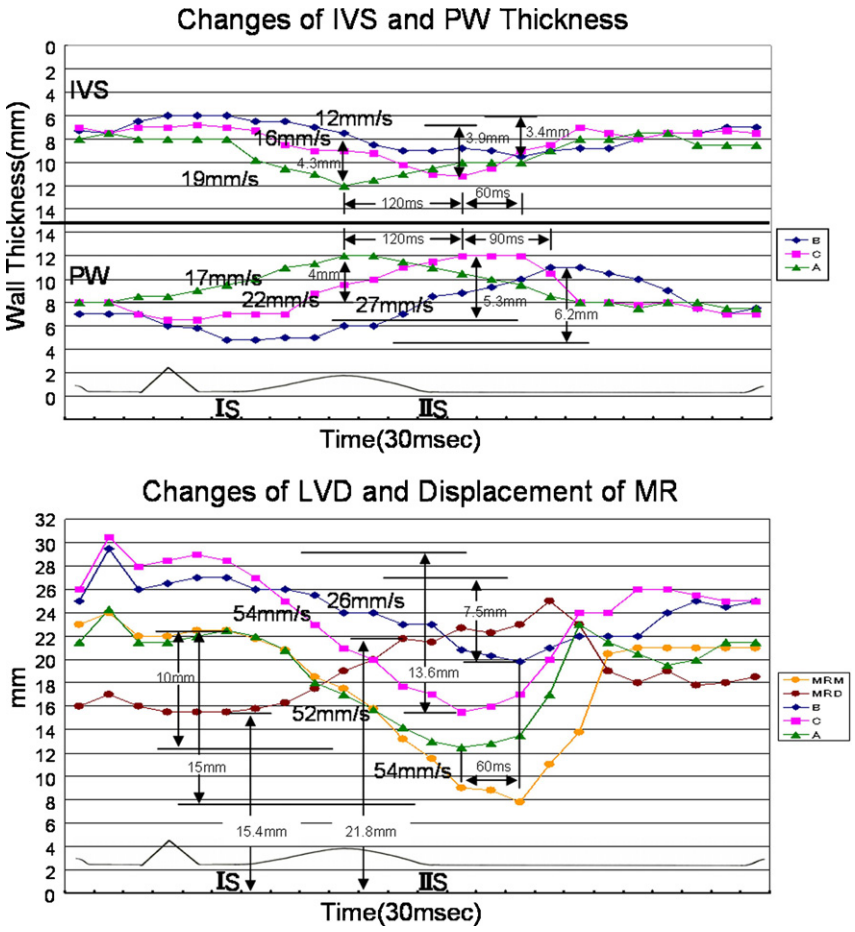

Figure 4 Top: changes in thickness of the posterior wall (PW) and the septum (IVS) at the basal (B, blue line), central (C, red line), and apical area (A, green line) of the LV during one cardiac cycle. Bottom: changes in internal diameter of the LV at the basal (B), central (C) and apical (A) area as well as the mitral ring (MRD). MRM changes in the distance of down ward displacement of the posterior part of mitral ring during one cardiac cycle. The number shows a speed of the change. Is: 1st heart sound, IIs: 2nd heart sound.

tole. In late systolic phase, this increased strain rate rapidly decreased in both RV and LV sides simultaneously.

Strain rate distribution in the PW (Fig. 6)

In the apical part, the strain rate remarkably increased in early systolic phase and the large stain rate area spread from the epicardial side to the endocardial side, resulting in the progressive thickening from the early stage of systole from the outer side to the inner side of the PW. Up to just before the end of systolic phase (judged by the second heart sound: S2), there were mixed large and small areas of the strain rate. There was a tendency to increase in the inner half, whereas to decrease in the outer half of the myocardium, indicating the persisting contraction in the former and relaxation or extension in the latter portion. The strain rate in the apical part decreased markedly in the end of systolic phase, resulting in the relaxation or dilatation. The strain rate in the central to basal parts temporarily decreased markedly in the beginning of systolic phase, giving rise to the decrease in the thickness of the myocardium and dilatation of the LV cavity.

The increase in the strain rate in the basal part spread to the isovolumetric relaxation beyond the timing of the S2. From the end-systolic phase to the isovolumetric relaxation period, the basal part showed the inner half having increasing strain rate and the outer half having decreasing strain rate simultaneously, indicating the simultaneous appearance of thickening of the inner half and extension or thinning of outer half. In the middle of central part, there was the area where neither extension nor contraction occurred due to the stratified coexistence of increase and decrease in the strain rate.

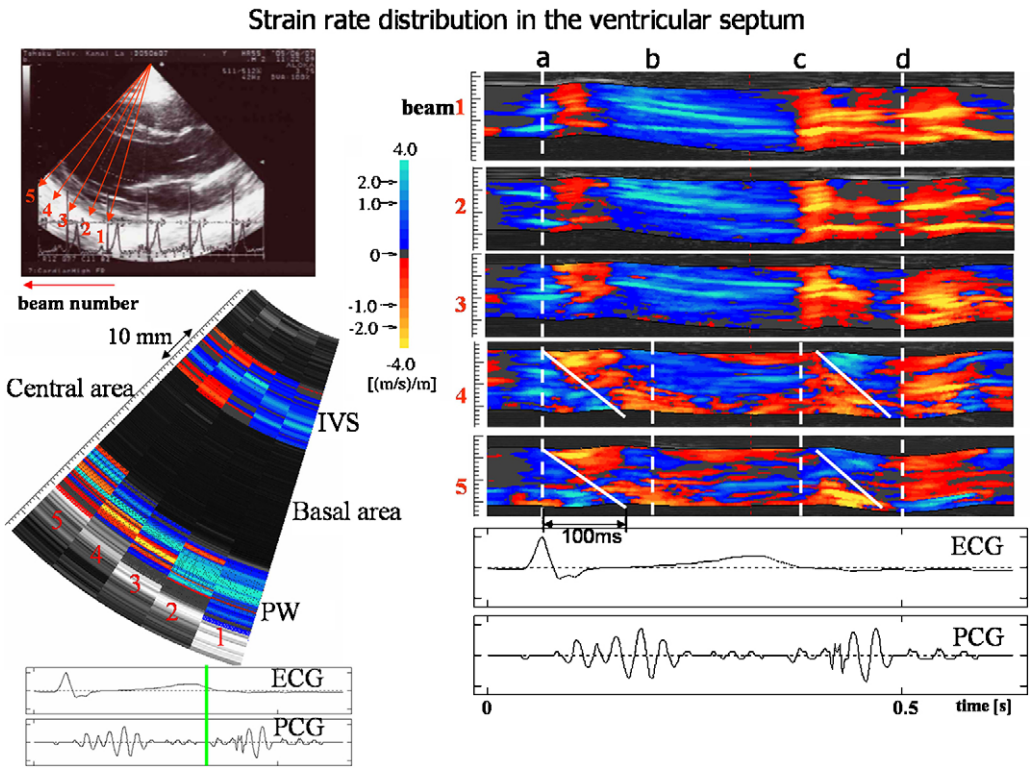

Figure 5 M-mode images of a time sequential change of the strain rate distribution in the interventricular septum (IVS) measured by sparse scan method on the longitudinal section plane of the LV during one cardiac cycle is shown. The M-mode display of the strain rate of 1—5 correspond to those of 2D echo-cardiogram in the left row. Left middle figure shows 2D strain rate image in the time point of the green line in the ECG.

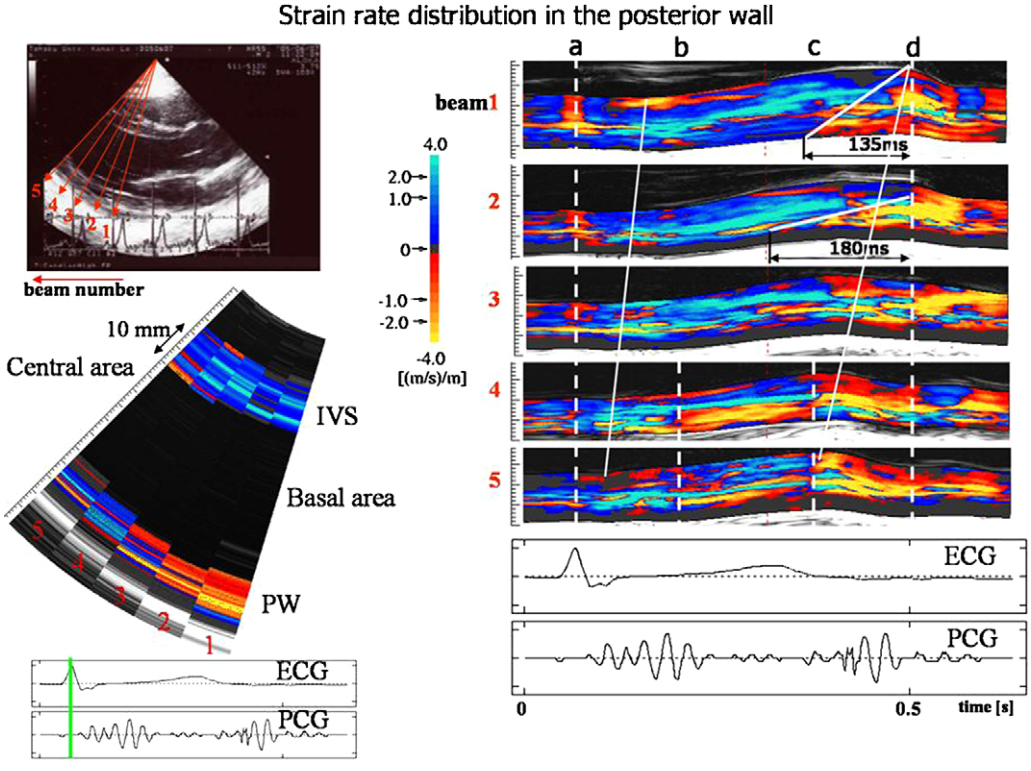

Figure 6 M-mode images of a time sequential change in the strain rate distribution of the posterior wall (PW) measured by the same method as in Fig. 5.

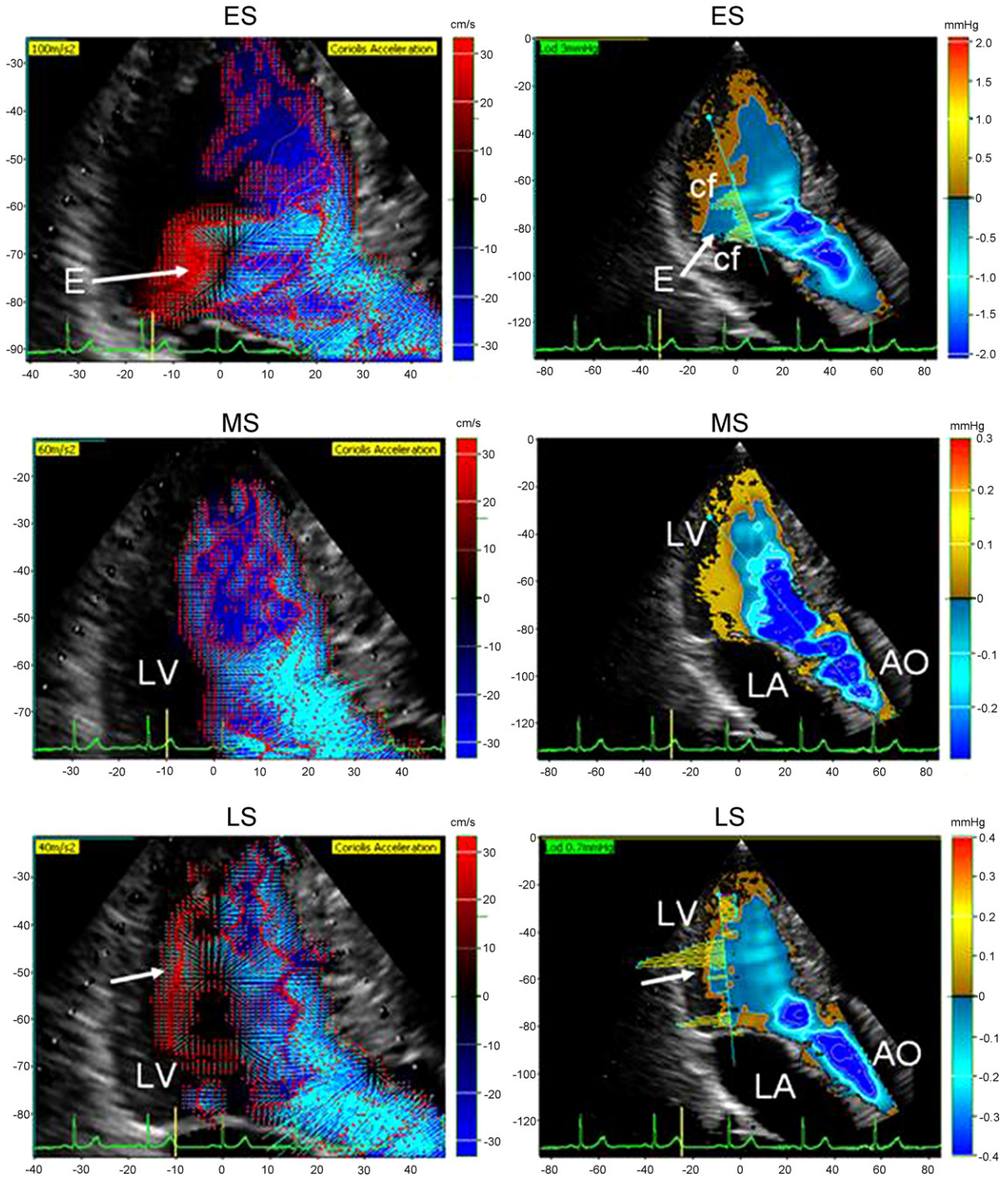

Figure 7 Left column: 2D distribution of the acceleration for changing the flow direction in the LV in the early systole (ES), mid-systole (MS), and late systole (LS). The acceleration vector (blue line) is localized in the outflow area in ES, and the eddy shows a radial pattern (E: white arrow). In MS, the stratified distribution appeared perpendicular to the inner surface of the PW and IVS. In LS, the stratified distribution is seen perpendicular to the IVS and small radial distribution (white arrow) indicating the eddy shows in the apical area. Right column: 2D distribution of the Doppler pressure in the LV. Cold color area shows a negative pressure and warm color area, positive pressure. In ES, the negative pressure caused by the eddy (E) appears in the basal area near the mitral valve. In LS, the negative pressure (white arrow) spread and appeared at the area adjacent to the basal and central parts of the PW indicating the occurrence of the premature dilatation and the beginning of the sucking action of the LV.

Systolic flow dynamics evaluated by 2D distribution of the acceleration for changing the flow direction

Distribution of the acceleration vector for changing the flow direction within the LV is demonstrated in the left column of Fig. 7.

In the early systolic phase, stratified pattern of acceleration appeared at the basal area near the IVS. At the same time, radial pattern (E) of acceleration caused by the eddy was observed just behind of the anterior mitral valve (Fig. 7-ES). In the mid-systolic phase, the direction of acceleration vectors showed perpendicular from the inner surface of the IVS and PW and the distribution was observed from apical to basal area indicating the distribution of the force produced in the short-axis direction by wall contraction (Fig. 7MS). In the mid- and late systolic phase, the line drawing with the tip of the acceleration vector showed parallel to the inner surface of the IVS and PW, showing the wave pattern. In the late systolic phase (Fig. 7LS), two small radial patterns of the acceleration vector were observed at the central and apical area near the PW (white arrow) indicating production of the small eddy. At the same time, the arrangement of the tip of the vector showed the flat pattern parallel to the inner surface of the PW and the vectors in the inflow tract area mainly directed to the PW indicating the outward expansion of the PW nevertheless the direction of vectors in the adjacent area to the IVS showed perpendicular from the inner surface of the IVS.

2D Doppler pressure distribution in the systolic phase

2D Doppler pressure distribution is demonstrated in the right column in Fig. 7.

Throughout systole, high pressure area in the LV was adjacent to the PW from the apical to basal part, whereas low pressure area was in the outflow tract and in the basal area of the aorta beyond the valve. The lowest Doppler pressure was about −11 mmHg just under the aortic valve.

The pressure distribution in the eddy flow behind the anterior mitral leaflet in the early systolic phase was about −0.3 mmHg at the center of the eddy and −0.8 mmHg at the circumferential part. Thus the eddy in the early systolic phase was in the developing stage (Figs. 7ES and 2-2). In the late systolic phase, the negative pressure appeared again at the basal to apical area adjacent to PW (white arrow in Fig. 7-LS) due to the premature relaxation and extension of the ventricle indicating the beginning of the sucking action.

Discussion

Since the advent of modern cardiology, cardiac function has been evaluated by global measurements, such as cardiac output, ejection fraction, total flux and pressure and many others [21—23]. However, these are inadequate because of the lack of the local information of the heart and blood flow.

Using non-invasive technology, we need the following three measurements for the clinical purpose. These are:

(1) blood flow structure and flow dynamics in cardiac chambers,
(2) mechanical events of cardiac structure during pulsation,
(3) local myocardial function of the LV.

For these purposes, several trials using computer analysis [24—26] or X-ray ventriculography [10,27] have developed, but these are not available at the bedside. Recent clinical methodology, such as ultrasonic method [28—30] or magnetic resonance imaging (MRI) [31,32], has been proposed, but the former has a difficulty to obtain the vector value of blood flow velocity and the latter is not enough to analyze flow dynamics because of the limited spatial resolution.

Present report deals with the analysis of above-mentioned three informations using echo-dynamography, strain rate analysis with sparse scan technique and high frame rate echo-tomography to clarify the following four systolic phenomena.

(1) characteristics of the blood flow structure in the LV and its generation mechanism,
(2) correlation between the flow structure and mechanical events of the ventricular wall,
(3) correlation among the flow structure, flow dynamics and pump function,
(4) asynchronism in myocardial contraction for generating the flow structure.

Characteristics of the flow structure of the intra-ventricular flow during the systolic phase and its generation mechanism

Characteristics of the blood flow structure in the intraventricular flow during systole are summarized as shown in Fig. 8. The blood flow passing through the outflow tract area during systole was laminar and the flowing structure showed a plane symmetry to the longitudinal section plane which includes the

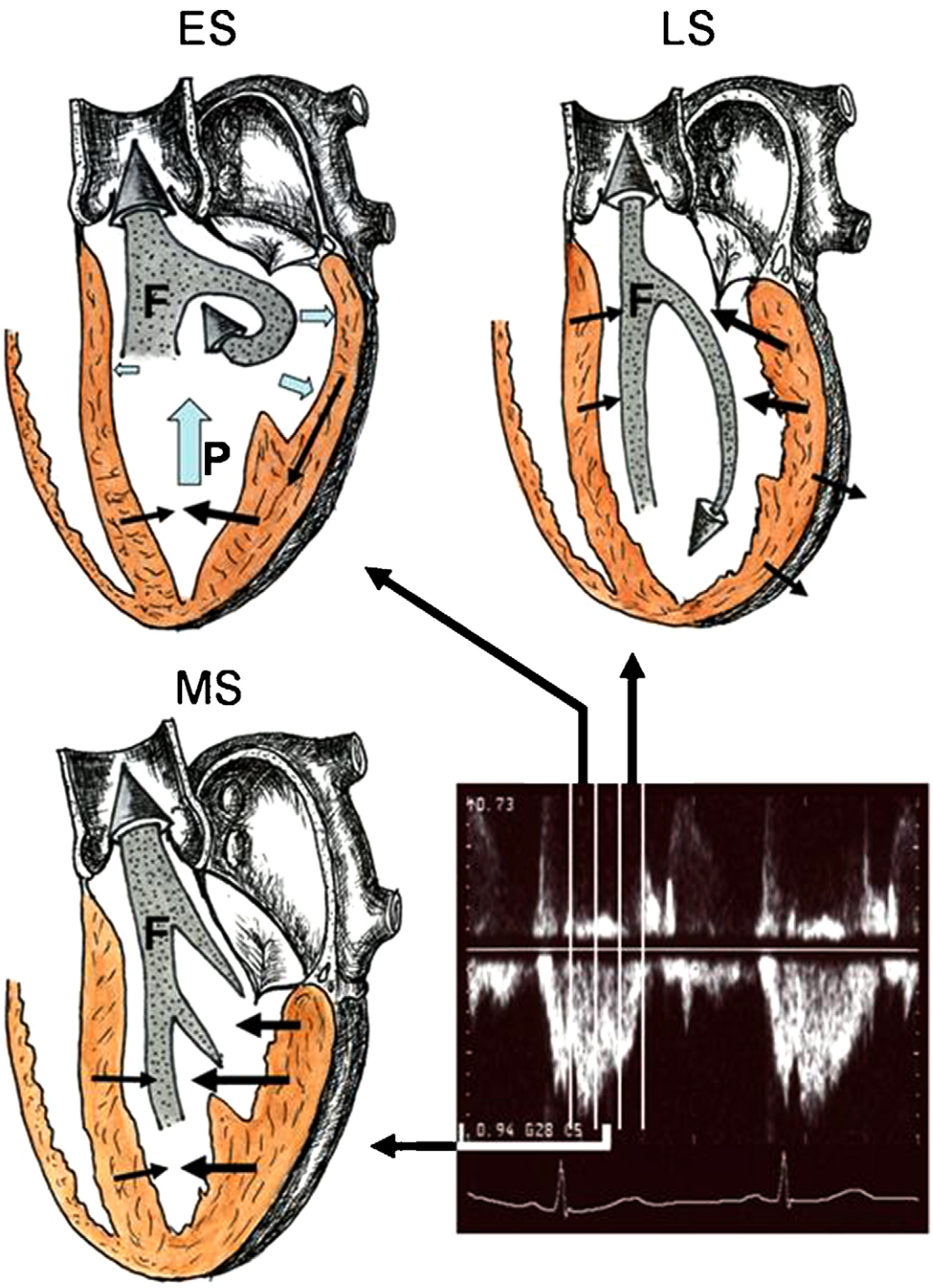

Figure 8 Schematic representation of the flow structure in the early, mid- and late systolic phase and summarized correlation among the flow structure, flow dynamical changes and ventricular wall dynamics during systolic phase. Gray arrow (F): flow structure, Black arrow in figures: direction and magnitude of the wall movement, Blue arrow (P): dynamic pressure, Right under picture shows the Doppler flow velocity curve obtained in the outflow tract of the LV, and correlation between timing of the schematic flow pattern and real flow is represented.

long axis line of the LV. As demonstrated in Fig. 8, the blood in the basal area in the early systolic phase (ES) begin to move to the aorta, and at the same time, a part of the blood in the basal area moved toward posteriorly along the mitral valve and produced an accelerated eddy at the area adjacent to the ventricular surface of the MV. In the mid-systolic phase (MS), the flow speed in the apical and central area gradually increased while being gathered the blood in the inflow area near the PW to

the outflow area near the IVS. The flow velocity in the inflow tract area remarkably decreased. In the late systolic phase, the speed of the ejected flow was obliged to decelerate. At this time, some part of the blood flow separated from the main flow at the basal area and moved downward to the apical area along the PW and a rotating flow appeared in the posterior half area of the LV together with small eddies at the apical area. Thus, the flow structure in the systolic phase had respective characteristics in the early, mid- and late systolic period, respectively.

The flow structure is produced by the changes in the regional wall motion and wall dynamics during ventricular pulsation. The investigation disclosed the following characteristics concerning mechanical phenomena; i.e.

(1) The LV short-axis transformation occurred together with deduction of the internal diameter, and the increase in the predominant PW thickness propagated from the apical to basal region (peristaltic squeezing).
(2) The LV long-axis transformation occurred together with the anterior displacement of the PW with protrusion of the papillary muscle. The plane encircled by the mitral ring had hinge-like movement. The fibrous trigone act as a fulcrum and downward movement of the posterior part of the ring changed the shape from elliptic to circular with an increment of the surface area.
(3) Diminished volume and short-axis diameter of the LV caused by (1) and (2) modes was followed by the shift of the main flow axis line toward the IVS during systole. This is a bellows action.
(4) Dimensional changes of the funnel-shaped outflow tract which was formed by the basal IVS, the anterior leaflet of the mitral valve and the basal PW.

Based on the flow structure and the mode of wall dynamics above-mentioned, the possible mechanism of ventricular ejection is as follows:

As summarized in Fig. 8, at the beginning of ventricular contraction, peristaltic motion (mode (1)) starts at the apical part with mode (2) ventricular transformation, high pressure at the apical area is transmitted the basal area and ejects the blood. Simultaneously, the basal part of LV is expanded posteriorly in a short period following isovolumetric contraction, and consequently some parts of blood move posteriorly along the mitral valve. The bellows action of the mode (3) helps the development of the forceful accelerated vortex with equal dispersion of the centrifugal force, which causes the smooth closure of the mitral valve as pointed by Bellhouse [33] and Reul [34].

In mid-systole and later on, bellows action is emphasized. Namely, the ejected flow is generated by mechanical events (mode (3) and (4)).

At the later half of ejection period, myocardial thickness successively increased from apical to basal part as shown in the data of wall dynamics and strain rate distribution. Furthermore, the greater displacement of the wall occurred at the PW rather than IVS in the short-axis direction, all contribute blood flow toward outflow tract. Such a wall motion seems to maintain the completeness of ejection and proceeds to the closure of the aortic valve.

Rushmer [35] and Sakuma [36] described the important role of bellows action to the effective right ventricular ejection, while our present data indicated that the combined role of peristaltic action as well as bellows action of the ventricular wall is important for the completeness of systolic ejection in the LV.

In late systole, progressing the increment of the myocardial thickness at the basal part of the PW accompanying with the inward displacement, the posterior part of the mitral ring is made to move antero-upward and the antero-posterior diameter of the mitral ring diminish. At the same time, tension in the myocardium at the apical and central area is relieved in spite of the ejection period, and the premature relaxation and extension of myocardium begin and the LV tends to dilate (beginning of the sucking action).

The premature relaxation and extension produce the negative pressure in the area adjacent to the PW. At the same time, the negative pressure will act not only for generating the small eddies at the apical area but also for dragging posteriorly about one-thirds to one-sixth of the maximal flux during early phase of ejection, and gives rise to the rotating flow at the central area, which works as a brake to the ejecting force along the main flow axis line. Thus the velocity vector of the ejecting flow becomes nearly the same size from the apical to basal area and the successive ejecting flow is obliged to be moved solely by inertia.

Correlation between the blood flow structure and pump function of the heart

Acceleration process for ejecting blood from the LV is essential for evaluating myocardial function, however, it is difficult to understand the mechanism of acceleration using sole pressure gradient between the LV and aorta. We have to know spatial distribution of the force and magnitude of the force generated. The spatial distribution of the force in the LV will be reflected in the centralization of the

blood flow in the ventricle. The centralization of the flow is evaluated in the flow axis distribution. The magnitude of the force will be reflected in the magnitude of the acceleration of the blood flow and the acceleration mode. In this study, we analyzed acceleration mechanism, ventricular wall dynamics and their correlation based on the four items, i.e.

(1) two-dimensional distribution of the flow axis line of the ejecting blood flow,
(2) the velocity vector distribution on the main flow axis line and the velocity gradient along the main flow axis line,
(3) their transition (time course) during the systolic phase,
(4) two-dimensional distribution of the acceleration for changing the flow direction.

Summarized results demonstrated in Figs. 1 and 8. We found three kinds of acceleration modes along the flow axis lines; accelerations A, B and C. The ventricular ejection is accomplished by the combination of these three modes acceleration generated along the blood flow axes (Figs. 1 and 3).

Acceleration A was produced along the main flow axis line from the apical to outflow tract area of the LV. Two kinds of branched flow axes joined at the central and basal areas. The velocity gradient along the main flow axis line in the central area was about twice than that in the apical one and the gradient in the basal area about four times further than that in the apical ones. Thus, the acceleration increased at the central area, and further at the basal area (Fig. 3). This type of acceleration was generated by the wall dynamical mode 3.

Acceleration B, which appeared at the basal area parallel to the anterior leaflet of the mitral valve and generated by passing though the funnel structure constructed by the IVS, mitral leaflet and posterior wall, joined to the main flow axis line. Because of the extremely large antero-posterior diameter at the basal area compared with that of the aortic ostium, the convective acceleration generated becomes very large. This type of acceleration was generated by the wall dynamics modes 2 and 4.

Acceleration C, which observed along the circular flow axis line just behind the anterior mitral leaflet joined with the main flow axis line at the central area is essentially due to the high speed rotating flow. The centrifugal force is proportion to square of the rotation speed and is inverse proportion to the radius of rotation. Accordingly, accompanying decrease in the radius of rotation as in the early systolic period, the centrifugal force caused will be increased remarkably. The blood in the adjacent area is dragged into the accelerated rotation flow and thus the accelerated outflow is produced in the central area.

In the early systolic phase, all three modes work, and the acceleration increase about two times in the central area and about four times in the basal area compared with that in the apical area along the main flow axis line. In the mid-systolic phase, the acceleration A and B work, and the velocity gradient is about 1.3 times in the central area and about 3 times in the basal area compared with the velocity gradient in the apical area. In the late systolic phase, only B is active, so that the velocity gradient decreases and the flow velocity keeps nearly the same level according to the inertia.

From the 2D distribution of the flow axis line and the velocity gradient and acceleration distribution on the flow axis line, it is concluded that the pump function including the local function can be evaluated from the non-invasive information of blood flow structure.

Significance of the asynchronism in the myocardial contraction and extension for generating the flow structure

As indicated by the distribution of the velocity vector and the main and branched flow axis lines, both contracting and relaxing states coexisted simultaneously during ventricular systole, as indicated by the simultaneously contracting the apical part and relaxing basal part at the early systole and the reverse was true in the late systole.

The time difference of the wall thickness and internal diameter of the LV, and also the peristaltic squeezing and bellows action indicated that the myocardial contraction and relaxation in the local part have time discrepancy and also myocardial asynchrony always exist even during systole in the microscopic point of view by the strain rate distribution.

Furthermore, the strain rate distribution indicated that the reverse strain rate occurred in early systole, resulting contraction of the apical part and relaxation of the basal part. Even though, myocardial wall has laminar layer, positive strain rate in the inner half of contraction accompanied with negative rate in the outer half of relaxation and thus the wall thickness change propagated from epicardial to endocardial side.

From these facts, asynchronism of myocardial contraction and the time discrepancy of the asynchrony among local parts seems to play an important roll in the smooth intra-ventricular blood flow and the effective pump function of the LV.

Conclusions

Systolic blood flow in the left ventricle analyzed by using the echo-dynamography was the laminar flow along the interventricular septum. The flow structure is quite different in its character in such cardiac phases as early, mid- and late systole and was produced by the wall dynamic events such as peristaltic squeezing of the ventricular wall, hinge-like movement of the mitral valve ring plane, bellows action and dimensional change in the funnel shape of the basal part of the LV. Concerning the correlation between the flow structure and pump function, distribution of the force in the LV is reflected on the flow axis line distribution, and the flow acceleration composed of three varieties, i.e., A: from apex to outflow along the main flow line, B: along the mitral leaflet, and C: vortex at the mitral valve. Even during systole, macroscopic and microscopic asynchronous contraction and relaxation in local part of the wall contribute to not only the generation of the flow structure but also the smooth and effective pump function.

References

[1] Tanaka M. Historical perspective of the development of echocardiography and medical ultrasound. In: Schneider SC, Levy M, McAvoy BR, editors. Proceedings of the IEEE ultrasonics symposium, vol. 2. New York: IEEE Inc.; 1998. p. 1517—24.

[2] Tanaka M, Nitta S, Yamamoto A, Takahashi K, Saijo Y, Ohtsuki S. Development and application of non-invasive method for the evaluation of cardiac function, quantifying intracardiac blood flow. Asian Med J 1994;37:283—6.

[3] Tanaka M, Nitta S, Yamamoto A, Sato N, Takahashi K, Saijo Y, et al. Development and application of non-invasive methods for the evaluation of cardiac function. Measuring cardiac function. Asian Med J 1994;37:397—400.

[4] Tanaka M, Nitta S, Yamamoto A, Takahashi K, Saijo Y, Ohtsuki S. Development and application of non-invasive method for the evaluation of cardiac function: visualization of pressure changes in heart chambers. Asian Med J 1994;37:341—4.

[5] Tanaka M, Ohtsuki S, Sugawara S. Quantitative visualization of the blood flow in heart chambers by means of the two dimensional stream line distribution method. In: Proceedings of the comput visual symposium. Tokyo: Nikkei Science; 1998. p. 1—4 [in Japanese].

[6] Ohtsuki S, Tanaka M. The flow velocity distribution from the Doppler information on a plane in three dimensional flow. J Visual 2006;9:69—82.

[7] Hino M. Introduction to fluid mechanics. Tokyo: Asakura Boock Co.; 2002. p. 82—86.

[8] Ohtsuki S, Tanaka M. Flow function for streamlines representative of the flow on a plane in three-dimensional flow. J Visual Soc Jpn 1998;18:136—40 [in Japanese].

[9] Nakajima H, Tanaka M, Sugawara S, Katahira Y, Ohtsuki S. Clinical significance of the velocity distribution on the flow axis line for evaluating the left ventricular function. J Cardiol 2004;44(Suppl):428 [abstract].

[10] Schoephoerster RT, Silva CL, Ray G. Evaluation of left ventricular function based on simulated systolic flow dynamics computed from regional wall motion. J Biomech 1994;27:125—36.

[11] Tanaka M, Kanai H, Sato M, Chubachi N. Measurement of the moving speed of local myocardial tissue by using the phase difference tracking method and its clinical significance. J Cardiol 1996;28(Suppl):163 [abstract].

[12] Kanai H, Hasegawa H, Chubachi N, Koiwa Y, Tanaka M. Noninvasive evaluation of local myocardial thickening and its color-coded imaging. IEEE Trans Ultrson Feroelect Freq Contr 1997;44:752—68.

[13] Kanai H, Hasegawa H, Chubachi N, Koiwa Y, Tanaka M. Non-invasive evaluation of spatial distribution of local instantaneous strain energy in heart wall. In: Lees S, Ferrari LA, editors. Acoustic imaging, 23. New York: Plenum Press; 1997. p. 187—92.

[14] Sugawara S, Tanaka M, Katahira Y, Nakajima H, Ohtsuki S. Development of echo-dynamography (blood flow analysis by acceleration distribution method). Jpn J Med Ultrason 2004;31(Suppl):S-167 [in Japanese].

[15] Sugawara S, Tanaka M, Katahira Y, Nakajima H, Ohtsuki S. Clinical significances of an arrangement pattern of the tip of acceleration vector of the blood flow in left ventricle and aorta. J Cardiol 2004;44(Suppl):464 [abstract in Japanese].

[16] Tanaka M, Sugawara S, Ohtsuki S. Non-invasive measurement of the pressure distribution at the local area in heart chambers and its clinical significances. J Cardiol 1999;34(Suppl I):413 [abstract in Japanese].

[17] Sugawara S, Tanaka M, Nitta K, Katahira Y, Ohtsuki S. Doppler pressure distribution method for non-invasive evaluation of the cardiac pump function. J Cardiol 1999;34(Suppl I):103 [abstract in Japanese].

[18] Tanaka M, Sugawara S, Nitta K, Nakajima H, Ohtsuki S. Characteristics of the Doppler pressure distribution in the systolic phase in the pressure over load diseases. J Cardiol 2001;38(Suppl I):130 [abstract in Japanese].

[19] Ohtsuki S, Tanaka M. Doppler pressure field deduced from the Doppler velocity field in an observation plane in a fluid. Ultrasound Med Biol 2003;29:1431—8.

[20] Tanaka M, Takahashi K, Saijo Y, Chiba S, Sasaki H, Mitsuoka M, et al. Analysis of the eddy flow appeared in the left ventricle in human heart. In: Nakayama Y, Takahashi T, editors. Proceedings of the 3rd Asian symp visualiz (ASV'94); 1994, Visual Soc Jap. p. 826—9.

[21] Braunwald E, Sonnenblick EH, Ross Jr J. Contraction of the normal heart. In: Braunwald E, editor. Heart disease. 2nd ed. Philadelphia, Tokyo: WB Saunders Co.; 1984. p. 409—46.

[22] Ishida N, Takishima T. Cardiodynamics and its clinical application. 2nd ed. Tokyo: Bunkodo Co.; 1992.

[23] Suga H. Cardiac Pumping capability in aspects of cardiac output-arterial pressure relations. The Saishin-Igaku 1975;30:1176—84 [in Japanese].

[24] Yoganthan AD, Lemmon Jr JD, Kim YH, Walker PG, Levin RA, Vesier CC. A computational study of a thin-walled three-dimensional left ventricle during early systole. J Biomech Eng 1994;116:307—14.

[25] Taylor TW, Okino H, Yamaguchi T. Three-dimensional analysis of left ventricular ejection using computational fluid dynamics. J Biomech Eng 1994;116:127—30.

[26] Gonzalez E, Schoephoester RT. A simulation of three-dimensional systolic flow dynamics in a spherical ventricle: effects of abnormal wall motion. Ann Biomed Eng 1996;24:48—57.

[27] Back LH, Gordon DG, Ledbetter DC, Selzer RH, Crawford DW. Dynamical relations for left ventricular ejection: Flow rate, momentum, force and impulse. J Biomech Eng 1984;106:54—61.
[28] Tanaka M, Okujima M, Ohtsuki S, Terasawa Y, Konno K, Ebina T. Non-invasive measurement of the blood flow velocity and of velocity distribution in cardiac chambers and great vessels by a new Doppler flow meter system. In: White D, Brown RE, editors. Ultras in Med 3B, engineering aspects. New York: Plenum Press; 1977. p. 1263—77.
[29] Nimura Y, Matsuo H, Kitabatake A, Hayashi T, Asao M, Terao Y, et al. Studies on the intracardiac blood flow with a combined use of the ultrasonic pulsed Doppler technique and two dimensional echocardiography from a transcutaneous approach. In: White D, Brown RE, editors. Ultras in Med 3B, engineering aspect. New York: Plenum Press; 1977. p. 1279—89.
[30] Namekawa K, Kasai C, Tsukamoto M, Koyano A. Real time blood flow imaging system utilizing auto-correlation techniques. Ultras Med Biol 1983;203(Suppl 2).
[31] Kim WY, Walker PG, Pedersen EM, Poulsen JK, Oyre S, Houlind K, et al. Left ventricular blood flow patterns in normal subjects: A quantitative analysis by three-dimensional magnetic resonance velocity mapping. JACC 1995;26:224—38.
[32] Walker PG, Cranney GB, Grimes RY, Delatore J, Rectenwald J, Pohost GM, et al. Three-dimensional reconstruction of the flowin a human left heart by using magnetic resonance phase velocity encoding. Ann Biomed Eng 1996;24: 139—47.
[33] Bellhouse BJ. Fluid mechanics of a model mitral valve and left ventricle. Cardiovasc Res 1972;6:199—210.
[34] Reul H, Talukder N, Muller EW. Fluid mechanics of the natural mitral valve. J Biomech 1981;14:361—72.
[35] Rashmer RF. Cardiovascular dynamics. 4th ed. Philadelphia: Saunders; 1976.
[36] Sakuma M, Ishigaki H, Komaki K, Oikawa Y, Kato A, Nakagawa M, et al. Right ventricular ejection function assessed by cineangiography—importance of bellows action. Circ J 2002;66:605—9.